

# VHR-REA\_IT Dataset: Very High Resolution Dynamical Downscaling of ERA5 Reanalysis over Italy by COSMO-CLM

Mario Raffa <sup>1</sup>, Alfredo Reder <sup>1</sup>, Gian Franco Marras <sup>2</sup>, Marco Mancini <sup>3</sup>, Gabriella Scipione <sup>2</sup>, Monia Santini <sup>4</sup>  
and Paola Mercogliano <sup>1,\*</sup>

- <sup>1</sup> Fondazione Centro Euro-Mediterraneo sui Cambiamenti Climatici, Regional Model and Geo-Hydrological Impacts (REMHI) Division, Via Thomas Alva Edison, 81100 Caserta, Italy; mario.raffa@cmcc.it (M.R.); alfredo.reder@cmcc.it (A.R.)
  - <sup>2</sup> HPC Department, CINECA, Via Magnanelli 6/3, 40033 Casalecchio di Reno, Italy; g.marras@cinca.it (G.F.M.); g.scipione@cinca.it (G.S.)
  - <sup>3</sup> Fondazione Centro Euro-Mediterraneo sui Cambiamenti Climatici, Advanced Scientific Computing (ASC) Division, Via Augusto Imperatore 16, 73100 Lecce, Italy; marco.mancini@cmcc.it
  - <sup>4</sup> Fondazione Centro Euro-Mediterraneo sui Cambiamenti Climatici, Impacts on Agriculture, Forests and Ecosystem Services (IAFES) Division, Viale Trieste 127, 01100 Viterbo, Italy; monia.santini@cmcc.it
- \* Correspondence: paola.mercogliano@cmcc.it

**Abstract:** This work presents a new dataset for recent climate developed within the Highlander project by dynamically downscaling ERA5 reanalysis, originally available at  $\approx 31$  km horizontal resolution, to  $\approx 2.2$  km resolution (i.e., convection permitting scale). Dynamical downscaling was conducted through the COSMO Regional Climate Model (RCM). The temporal resolution of output is hourly (like for ERA5). Runs cover the whole Italian territory (and neighboring areas according to the necessary computation boundary) to provide a very detailed (in terms of space–time resolution) and comprehensive (in terms of meteorological fields) dataset of climatological data for at least the last 30 years (01/1989–12/2020). These types of datasets can be used for (applied) research and downstream services (e.g., for decision support systems).

**Dataset:** [https://doi.org/10.25424/cmcc/era5-2km\\_italy](https://doi.org/10.25424/cmcc/era5-2km_italy).

**Dataset License:** Data are protected by copyright. Distribution and communication of the data to the public are not allowed without the Fondazione CMCC's written authorization. Access to, consultation with, and reproduction of the data, in whole or in part, for personal use or institutional and research purposes is permitted, but not for commercial purposes and not with the intent to distribute, communicate, or to make them available to the public. CINECA, through the Highlander platforms, and CMCC are the only institutions with permission to distribute, communicate, or make the data available to the public.

Adapting and transforming the data to create derivative works based on them, exclusively for personal, institutional, and research purposes is permitted, but not for commercial purposes, on the condition that:

An adequate mention of paternity is recognized through the citation of this paper to provide a link to the dataset doi ([https://doi.org/10.25424/cmcc/era5-2km\\_italy](https://doi.org/10.25424/cmcc/era5-2km_italy));

It is indicated whether any changes have been made;

In allowing for the creation of derivative works, their use for commercial purposes is never permitted.

CMCC Foundation submits their data to adequate verification activities, however, CMCC Foundation does not assume responsibility for any inaccuracy or omission in them. CMCC Foundation is not responsible for the data and news published when processed by third parties and for the contents provided by any other site starting from such data. CMCC Foundation does not assume responsibility for any decision based on such data, which remains the sole responsibility of the user, nor for any loss or damage, direct or indirect, that may arise from their use.



**Citation:** Raffa, M.; Reder, A.; Marras, G.F.; Mancini, M.; Scipione, G.; Santini, M.; Mercogliano, P. VHR-REA\_IT Dataset: Very High Resolution Dynamical Downscaling of ERA5 Reanalysis over Italy by COSMO-CLM. *Data* **2021**, *6*, 88. <https://doi.org/10.3390/data6080088>

Academic Editor: Eric Vaz

Received: 22 June 2021

Accepted: 3 August 2021

Published: 9 August 2021

**Publisher's Note:** MDPI stays neutral with regard to jurisdictional claims in published maps and institutional affiliations.



**Copyright:** © 2021 by the authors. Licensee MDPI, Basel, Switzerland. This article is an open access article distributed under the terms and conditions of the Creative Commons Attribution (CC BY) license (<https://creativecommons.org/licenses/by/4.0/>).

**Keywords:** reanalysis; regional climate models; convection permitting model; Italian historical hourly climate dataset

## 1. Summary

The development of convection-permitting regional climate models (CP-RCMs, spatial resolution <4 km) is returning a step change in the ability to understand past climate and future climate change at local scales, supporting the characterization of extreme weather events that most impact society [1]. Some European initiatives (e.g., H2020 EUCP, CORDEX-FPS convection), as well as an increasing number of scientific works [2–11], have provided encouraging evidence for the improvement of CP-RCMs for the representation of hourly precipitation characteristics (i.e., diurnal cycle, spatial structure of precipitation, intensity distribution, and extremes [12]) towards dynamics matching reality. In addition, they have also brought out the capacity of CP-RCMs to detect surface heterogeneities (e.g., mountains, coastal regions, and urban areas; [2,7,13]), and a better feature of land–atmosphere feedback [14], which is necessary to preserve/amplify other extremes such as droughts or summer heat waves [15]. These improvements can also have a knock-on effect on other variables (e.g., energy fluxes such as latent heat and sensible heat, and soil moisture), usually scarcely monitored but of considerable interest for different types of applications. This is one of the major strengths of developing climate analyses on limited areas (e.g., specific countries) to support existing monitoring networks.

In this view, climate reanalysis represents a solution to ensure homogeneity and continuity of data for past and current climate, providing a comprehensive set of variables (in addition to traditional precipitation and temperature). Climate reanalysis “delivers a complete and consistent picture of the past weather” (<https://climate.copernicus.eu/climate-reanalysis>, accessed on 4 August 2021), relying on a numerical weather prediction model to assimilate historical observations (e.g., from satellite, in situ, multiple variables) that are not homogeneously distributed around the globe. Recently, the European Centre for Medium Range Weather Forecast (ECMWF) released the ERA5 reanalysis, currently representing the most plausible description for climate [16]. It has a global coverage with a native spatial resolution of  $0.28^\circ$  ( $\simeq 31$  km) and provides outputs at an hourly scale from 1950 to the present (with a latency of five days). Such features make ERA5 suitable for a wide range of applications, e.g., monitoring climate change, research, education, policy making and business, and in sectors such as renewable energy and agriculture [17].

A step forward is to bring the potential of ERA5 to the convection permitting (CP) scale with the aim of synergistically exploiting CP-RCM features and ERA5 reliability and creating new very-high resolution (VHR) climate dataset for past climate, using a model setup specific for areas of interest. This is the rationale adopted in the framework of the HIGHLANDER project (<https://highlanderproject.eu/>, accessed on 4 August 2021) to create a new additional gridded dataset over Italy, labelled as VHR-REA\_IT (Very High Resolution REAnalysis for ITaly), derived from the dynamical downscaling of ERA5 reanalysis from their native resolution ( $\simeq 31$  km) to a resolution of  $\simeq 2.2$  km for the period 1989–2020.

The downscaling activity was performed by the Centro euro-Mediterraneo sui Cambiamenti Climatici (CMCC) Foundation exploiting the Consorzio Interuniversitario del Nord-Est per il Calcolo Automatico (CINECA) supercomputer cluster GALILEO. The outputs have been stored as NetCDF [18] files at CMCC Supercomputing Center facilities and they have been integrated into the CMCC data delivery system (DDS) (<http://dds.cmcc.it>, accessed on 4 August 2021). Through the DDS web user interface (UI), users can easily build queries related to the VHR-REA\_IT dataset, choosing from a list of available variables, selecting the geographical area of interest or a location, and/or the time period, and then, according to the selected criteria, users can retrieve data by using the DDS Python client (<https://anaconda.org/Fondazione-CMCC/ddsapi>, accessed on 4 August 2021). Data is

also available on the Highlander platform (<https://highlanderproject.eu/data>, accessed on 4 August 2021) and can be accessed in a similar manner.

The present work reports a general description of VHR-REA\_IT dataset, explaining the data production steps and outputs included in the dataset and providing some insights about a comparison performed with respect to state of the art datasets available over Italy (i.e., E-OBS gridded observations [19], and ERA5 parent reanalysis) to give a reference for potential users.

## 2. Data Description

### 2.1. Data Production

Data are produced by dynamical downscaling of ERA5 reanalysis at the convection permitting scale (horizontal grid spacing  $0.02^\circ$ ,  $\approx 2.2$  km) over the domain covering the Italian Peninsula (Lon =  $5^\circ$  W– $20^\circ$  E; Lat =  $36^\circ$  N– $48^\circ$  N) for the period from January 1989 to December 2020; the first year, 1988, is assumed to be a spin up. The downscaling activity is performed with the regional climate model COSMO model in CLimate Mode (COSCOSMO-CLM) [20] switching on the module TERRA-URB [21] to account for the urban parameterizations.

COSMO-CLM [20] is a non-hydrostatic, limited-area model designed for climate simulations at different horizontal resolutions varying from the meso- $\beta$  scale ( $\sim 20$ – $200$  km) to the meso- $\gamma$  one ( $\sim 2$ – $20$  km). Such a model exploits finite difference methods to solve the fully compressible governing equations of fluid dynamics on a structured grid. TERRA-URB [21] is a bulk scheme tailored for properly parameterizing urban physics in COSMO-CLM. Such a scheme makes use of a tile approach to discern for each grid cell between urban canopy and natural land cover and computes adjusted soil and water fluxes considering urban environment features.

Figure 1 displays the computational domain used for the downscaling activity while Table 1 reports the main features of the experimental configuration.

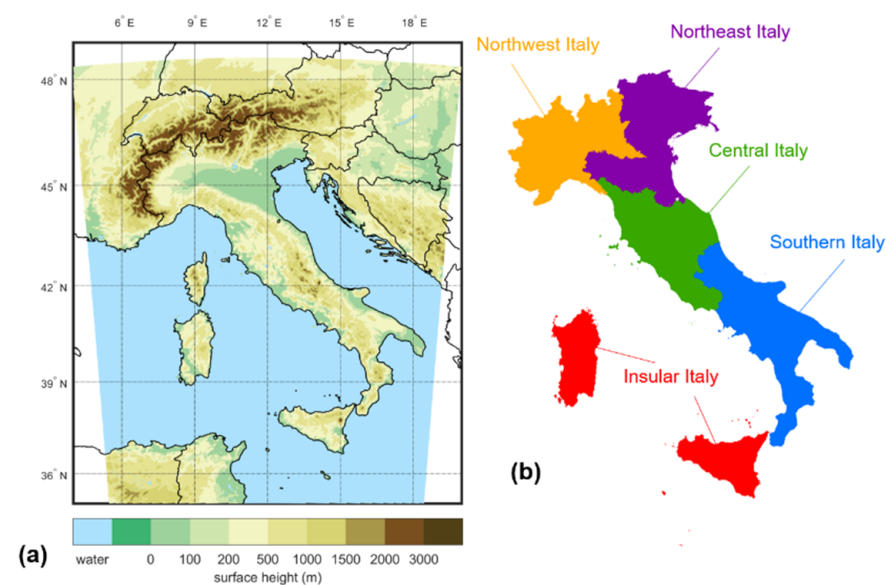


**Figure 1.** (a) Surface height (m a.s.l.); (b) area considered for technical validation, defined according to the first level of Nomenclature of Territorial Units for Statistics (NUTS 1) for Italy.

**Table 1.** Experiment configuration for VHR-REA\_IT data production [10].

| Boundary Forcing                                  | ERA5-Reanalysis   |
|---|---|
| Horizontal resolution                             | 0.02° ( $\approx 2.2$ km)   |
| Time step   | 20 s  |
| N° grid cells                                     | 585 × 730   |
| N° vertical levels                                | 50 (top model level elevation = 22 km)                                  |
| Output frequency                                  | 1 h   |
| Lateral sponge zone                               | 25 grid cells (on each horizontal boundary layer)                       |
| Radiation scheme                                  | Ritter and Geleyn [22]  |
| Convection scheme                                 | Shallow convection based on Tiedtke [23]                                |
| Microphysics scheme                               | Doms et al. [24]; Baldauf and Schulz [25]                               |
| Land surface scheme                               | TERRA-ML [20]<br>with TERRA-URB [21] parametrization                    |
| Land use  | GLC2000 [26]  |
| Planetary boundary layer scheme                   | Mellor and Yamada [27]  |
| Lateral Boundary Condition (LBC) update frequency | 3 h   |
| Soil initializations                              | Temperature and moisture obtained by interpolation from ERA5-Reanalysis |

The configuration derives from the COSMO-DE setup used by the Deutscher Wetterdienst (DWD) for numerical weather prediction application. It has also been adopted by several institutes acting in the Climate Limited-area Modelling-Community as a reference for climate mode experiments in the frame of the Coordinated Downscaling Experiment (CORDEX) [28,29] of the World Climate Research Programme (WCRP) for the Flagship Pilot Study (FPS) on convection [4]. Such an FPS focuses on the investigation of convective-scale events in a few key regions of Europe and the Mediterranean basin with convection-permitting regional climate models. To produce the VHR-REA\_IT dataset, the configuration has been properly configured by performing a series of sensitivity tests.

Formally, the default COSMO convective parameterization is the Tiedtke mass-flux scheme with moisture convergence closure [23]. Such a scheme distinguishes between shallow, deep, and midlevel convection. In the convection-resolving setup (i.e., that used for ERA5@2km), only the shallow convection part of the scheme is active, while for deeper clouds the scheme is turned off.

The setup was borrowed from the ERA5 evaluation downscaling experiments performed by Raffa et al. [10] over part of central Europe, including urban areas such as Cologne (Germany) and Paris (France). These experiments were performed to identify the most reliable nesting strategy to be adopted for localizing ERA5 climate signal at a convection permitting scale ( $\approx 2.2$  km) with COSMO-CLM. These sensitivity tests highlighted the advantages of direct nesting into ERA5 against the adoption of intermediate simulations.

## 2.2. Computing Resources

The climate run was performed by CMCC on the GALILEO supercomputer of CINECA, the Italian computing centre. CINECA, coordinator of the Highlander project, designed, set up, and made available all the necessary HPC and CLOUD infrastructure required. The hpc is equipped with 1022 36-core compute nodes. Each one contains two 18-core Intel Xeon E5-2697 v4 (Broadwell) at 2.30 GHz. All the compute nodes have 128 GB of memory.

The long-term run was performed using 60 nodes, corresponding to 2160 cores, and employed about 61 h to perform a 1-year simulation. The long-term simulation produced a large amount of data,  $\approx 8$  TB of output data and greater than  $\approx 70$  TB of forcing data, including the 3-dimensional boundary data needed for the downscaling.

### 2.3. Data Records

Hourly data from the downscaling at the very fine resolution of ERA5 reanalysis over Italy are on a rotated grid ( $\approx 2.2$  km, irregular/rotated pole grid). Their temporal coverage is 01/01/1989 00:00 to 31/12/2020 23:00. These data are provided in NetCDF format (dimensions = time, longitude, latitude, single vertical level) and generally on single levels (i.e., 2 or 10 m from surface depending on the selected variables) except soil moisture, which is available at seven soil levels (i.e., depth = 1, 3, 9, 27, 81, 243, or 729 cm from surface). The reference coordinate system is WGS84 (EPSG 4326). This information is summarized in Table 2.

**Table 2.** Overview of key characteristics of the VHR-REA\_IT dataset.

| Dataset Title                              | VHR-REA_IT: Downscaling at Very Fine Resolution of ERA5 Reanalysis over Italy by COSMO-CLM for 1989–2020  |
|--|---|
| Data type                                  | Model-generated data (numerical)—Re-analysis downscaling  |
| Dataset owner/provider                     | Fondazione Centro Euro-Mediterraneo sui Cambiamenti Climatici (CMCC)  |
| Dimensions                                 | time, longitude, latitude, single vertical level  |
| Data input format                          | NetCDF (Climate and Forecast (CF) Metadata Convention; <a href="http://cfconventions.org/">http://cfconventions.org/</a> , accessed on 4 August 2021) both for input and output format. Exceptions under CF are however compliant with the UNIDATA Common Data Model (CDM) to codify the Coordinate Reference System ( <a href="https://www.unidata.ucar.edu/software/netcdf-java/v4.6/CDM/index.html">https://www.unidata.ucar.edu/software/netcdf-java/v4.6/CDM/index.html</a> , accessed on 4 August 2021) |
| Data spatial structure                     | Rotated grid  |
| Temporal coverage                          | 01/01/1989 00:00 to 31/12/2020 23:00 (the 1 year spin up period 1988 is excluded)   |
| Temporal resolution                        | 1 h   |
| Spatial extent (Horizontal coverage)       | Latitude range: 36° N–48° N<br>Longitude range: 5° W–20° E  |
| Coordinate System                          | WGS84 EPSG 4326   |
| Spatial resolution (Horizontal resolution) | $\approx 2.2$ km $\times$ 2.2 km (irregular/rotated pole grid)  |
| Vertical coverage                          | Surface, 2 or 10 m from surface, or 1, 3, 9, 27, 81, 243, or 729 cm depth depending on the variable   |
| Vertical Resolution                        | All output variables are on single levels except soil moisture provided for 7 soil levels   |

In addition, Table 3 lists the variables provided by this dataset with a short description to support the users and interpret the convention of the meteorological fields. Such variables were selected for specific use cases to be conducted in the HIGHLANDER project, in which the time series of climate data will be further post-processed (e.g., spatio-temporal aggregation, combination into indices) and used, for instance as indicators and/or impact models concerning animal and human wellbeing, crop water requirements, land suitability for forests and crops, surface water availability and variability, and soil erosion (advancing what done in [30]).

**Table 3.** Overview and description of variables.

| Long Name   | Short Name | Units               | Description  |
|---|------------|---------------------|--|
| 2 m temperature                                   | T_2M       | K                   | Temperature of air at 2 m above surface  |
| 2 m dew point temperature                         | TD_2M      | K                   | Temperature to which the air, at 2 m above surface, would have to be cooled for saturation to occur  |
| Total precipitation                               | TOT_PREC   | kg m <sup>-2</sup>  | Accumulated liquid and frozen water, comprising rain and snow, that falls to the surface   |
| U-component of 10 m wind                          | U_10M      | m s <sup>-1</sup>   | Eastward component of the 10 m wind  |
| V-component of 10 m wind                          | V_10M      | m s <sup>-1</sup>   | Northward component of the 10 m wind   |
| 2 m maximum temperature                           | TMAX_2M    | K                   | Maximum temperature of air at 2 m above surface  |
| 2 m minimum temperature                           | TMIN_2M    | K                   | Minimum temperature of air at 2 m above surface  |
| mean sea level pressure                           | PMSL       | Pa                  | The pressure (force per unit area) of the atmosphere at the surface  |
| specific humidity                                 | QV_2M      | kg kg <sup>-1</sup> | The mass fraction of water vapor in (moist) air  |
| total cloud cover                                 | CLCT       | 1                   | Proportion of a grid box covered by cloud; cloud fractions vary from 0 to 1  |
| Surface Evaporation                               | AEVAP_S    | kg m <sup>-2</sup>  | Accumulated amount of water that has evaporated from the surface   |
| Averaged surface net downward shortwave radiation | ASOB_S     | W m <sup>-2</sup>   | Amount of solar radiation (also known as shortwave radiation) that reaches a horizontal plane at the surface (both direct and diffuse) minus the amount reflected by the surface (which is governed by the albedo)                       |
| Averaged surface net downward longwave radiation  | ATHB_S     | W m <sup>-2</sup>   | Thermal radiation (also known as longwave or terrestrial radiation) refers to radiation emitted by the atmosphere, clouds and the surface. This parameter is the difference between downward and upward thermal radiation at the surface |
| Surface snow amount                               | W_SNOW     | m                   | Liquid water equivalent thickness of surface snow amount   |
| Soil (multi levels) water content                 | W_SO       | m                   | Liquid water equivalent thickness of moisture content of soil layer  |

### 3. Methods

#### 3.1. Notes on the Comparison of VHR-REA\_IT against Gridded Observations and Other Reanalysis

In this section, the VHR-REA\_IT dataset is compared with a reference gridded observational dataset available over Europe, acknowledged as E-OBS [19,31], and with the parent ERA5 reanalysis [16]. Such a comparison is conducted in terms of precipitation and temperature at a daily scale for the period 1989–2020, for mean tendencies and extremes.

In brief, E-OBS represents a daily gridded European land-only observational dataset at a horizontal resolution of 0.1° (~11 km) relying on the “blended” time series from the station network of the European Climate Assessment & Dataset (ECA&D) project. It contains data for precipitation amount, mean/maximum/minimum temperature, relative humidity, sea level pressure, and surface shortwave downwelling radiation. Its latest version (Volume 23), delivered by Copernicus Climate Data Store, covers the period 1950–2020.

While E-OBS represents a valuable resource for climate research in Europe, some limitations in the dataset exist and taking it as reference does not mean it represents the reality but rather a useful independent product for comparison purposes [32]. Indeed, E-OBS data

are affected by the same constraints and limitations [9,33] that are typical of observational gridded datasets. Concerning precipitation, an averaging effect in precipitation magnitude (i.e., the lower the spatial resolution, the larger the smoothing effect) could occur, as well as underestimations at high elevation due to the precipitation lapse rate not being properly accounted for or induced by stations sparseness. For E-OBS, these limitations are recognized as underestimation (typically 10–20%) at high intensities (smoothing effect) and overestimation at low intensities (moist extension into dry areas), while systematic errors are more substantial for convective rainfall [33]. Moreover, by inspecting the spatial distribution of stations for Italy as reported in Cornes et al. [19], we can note how north Italy and the Po' Valley are well covered by stations for precipitation while the rest of the territory is characterized by a scarcity of measurements; such a scarcity is amplified in terms of stations for temperature measurements.

As a spatial reference, the Nomenclature of Territorial Units for Statistics (NUTS) classification is used to subdivide Italy into specific areas. Two levels of NUTS are considered: the former represents the whole Italian territory; the latter divides the Italian territory into five sub-areas (i.e., Northwest Italy, Northeast Italy, Central Italy, South Italy, and Insular Italy), identified in Figure 1b.

Specifically, the following issues are analyzed:

- 2 m temperature and total precipitation; this provides a general overview about the reliability of the new produced data in terms of mean patterns;
- a set of climate indicators related to extremes derived from a core set of extreme indices for temperature and precipitation provided by the experts of the CCI/CLIVAR/JCOMM Team on Climate Change Detection and Indices (ETCCDI), along with some relevant percentiles (see Table 4 for indicators related to precipitation and Table 5 for indicators related to temperature); these indicators turn data produced by climate models into significant information for impact studies, highlighting various characteristics of extremes, including frequency, amplitude, and persistence.

**Table 4.** List of considered indicators related to precipitation.

| Label  | Description  | Units                   |
|--------|--|-------------------------|
| CDD    | Maximum number of consecutive dry days (<1 mm)                               | days year <sup>-1</sup> |
| CWD    | Maximum number of consecutive wet days (≥1 mm)                               | days year <sup>-1</sup> |
| Rx1day | Maximum of daily precipitation   | mm day <sup>-1</sup>    |
| Rx5day | Maximum of 5-day accumulated precipitation                                   | mm 5 days <sup>-1</sup> |
| 90p    | 90th percentile of daily precipitation considering only the wet days (>1 mm) | mm day <sup>-1</sup>    |
| 99p    | 99th percentile of daily precipitation considering only the wet days (>1 mm) | mm day <sup>-1</sup>    |
| R10    | Number of days with precipitation ≥10 mm day <sup>-1</sup>                   | days year <sup>-1</sup> |
| R20    | Number of days with precipitation ≥20 mm day <sup>-1</sup>                   | days year <sup>-1</sup> |

**Table 5.** List of considered indicators related to temperature.

| Label    | Description   | Units                   |
|----------|---|-------------------------|
| ID       | Ice days—annual count of days when the daily $T_{\max} \leq 0$ °C         | days year <sup>-1</sup> |
| SU       | Summer days—annual count of days when the daily $T_{\max} \geq 25$ °C     | days year <sup>-1</sup> |
| FD       | Frost days—annual count of days when the daily $T_{\min} \leq 0$ °C       | days year <sup>-1</sup> |
| TR       | Tropical nights—annual count of days when the daily $T_{\min} \geq 20$ °C | days year <sup>-1</sup> |
| TXx      | Annual maximum value of daily $T_{\max}$                                  | °C                      |
| 90p tmax | 90th percentile of daily $T_{\max}$                                       | °C                      |
| 10p tmin | 10th percentile of daily $T_{\min}$                                       | °C                      |
| TNn      | Annual minimum value of daily $T_{\min}$                                  | °C                      |

Operatively, 2 m temperature and total precipitation are investigated at a seasonal scale, while the ETCCDI indices are calculated on a yearly basis. For these variables, data are first computed on a yearly basis and then averaged to obtain a climatological mean. Conversely, percentiles are obtained from the distribution representing the whole period.

### 3.1.1. Temperature

Figure 2 shows the seasonal spatial distribution of 2 m temperature computed for the period 1989–2020 with E-OBS, ERA5, and VHR-REA\_IT (the first three columns) on their relative native grids. The same figure also depicts the seasonal spatial distribution of 2 m temperature bias with ERA5, and VHR-REA\_IT (the last two columns), assuming E-OBS as a reference. For bias representation, data have been interpolated onto a coarser grid (i.e., the one of ERA5) considering a constant lapse rate of  $-6.5 \text{ K}\cdot\text{km}^{-1}$  to account for differences in the elevation of grid cells.

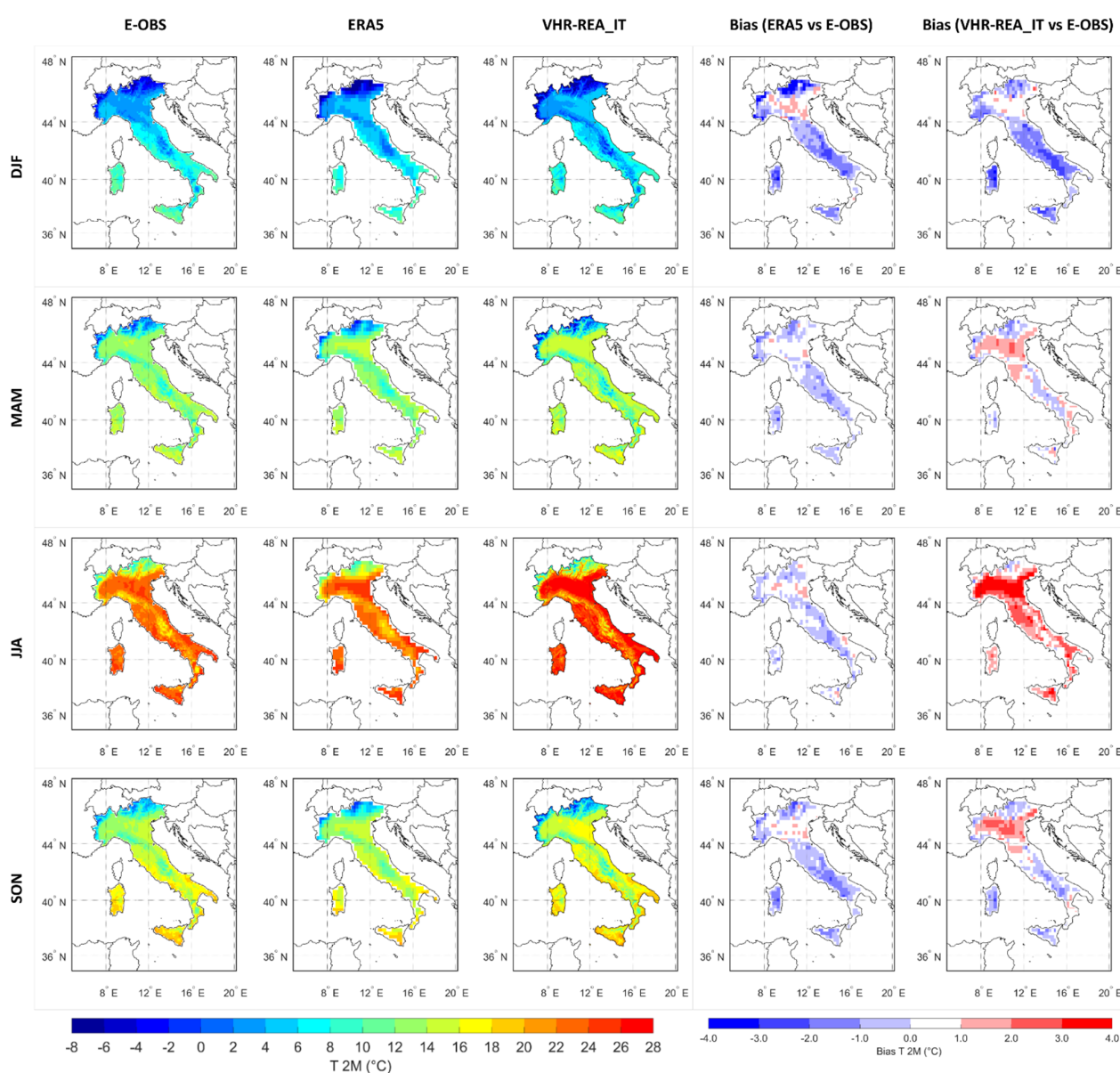


**Figure 2.** The first three columns: Seasonal (in row) spatial distribution of 2 m temperature for the period 1989–2020 provided by E-OBS, ERA5, and VHR-REA\_IT (in column); the last two columns: Seasonal (in row) spatial distribution of 2 m temperature bias for the period 1989–2020 provided by ERA5 and VHR-REA\_IT (in column) assuming E-OBS as a reference.



Italy (+1.2 °C). The transitional seasons (autumn and spring) show a slight warm bias; such a bias is because of temperatures during early autumn and late spring.

In general, VHR-REA\_IT benefits—with respect to ERA5—from the use of CPS, mainly for the refinement of the orography (as is noticeable from an analysis of the temperature in northern Italy, especially if the northwest or winter are considered). Further investigations will be performed in this sense. Finally, in terms of spatial variability, the analysis of standard deviation returns a good agreement with observations. This is expected, as temperature represents quite a homogeneous field.

### 3.1.2. Precipitation

Figure 3 depicts the seasonal spatial distribution of daily precipitation computed for the period 1989–2020 with E-OBS, ERA5, and VHR-REA\_IT (the first three columns) on their relative native grids. The same Figure also shows the seasonal spatial distribution of 2 m temperature bias with ERA5 and VHR-REA\_IT (the last two columns) assuming E-OBS as a reference. In this case, no correction for elevation has been applied.

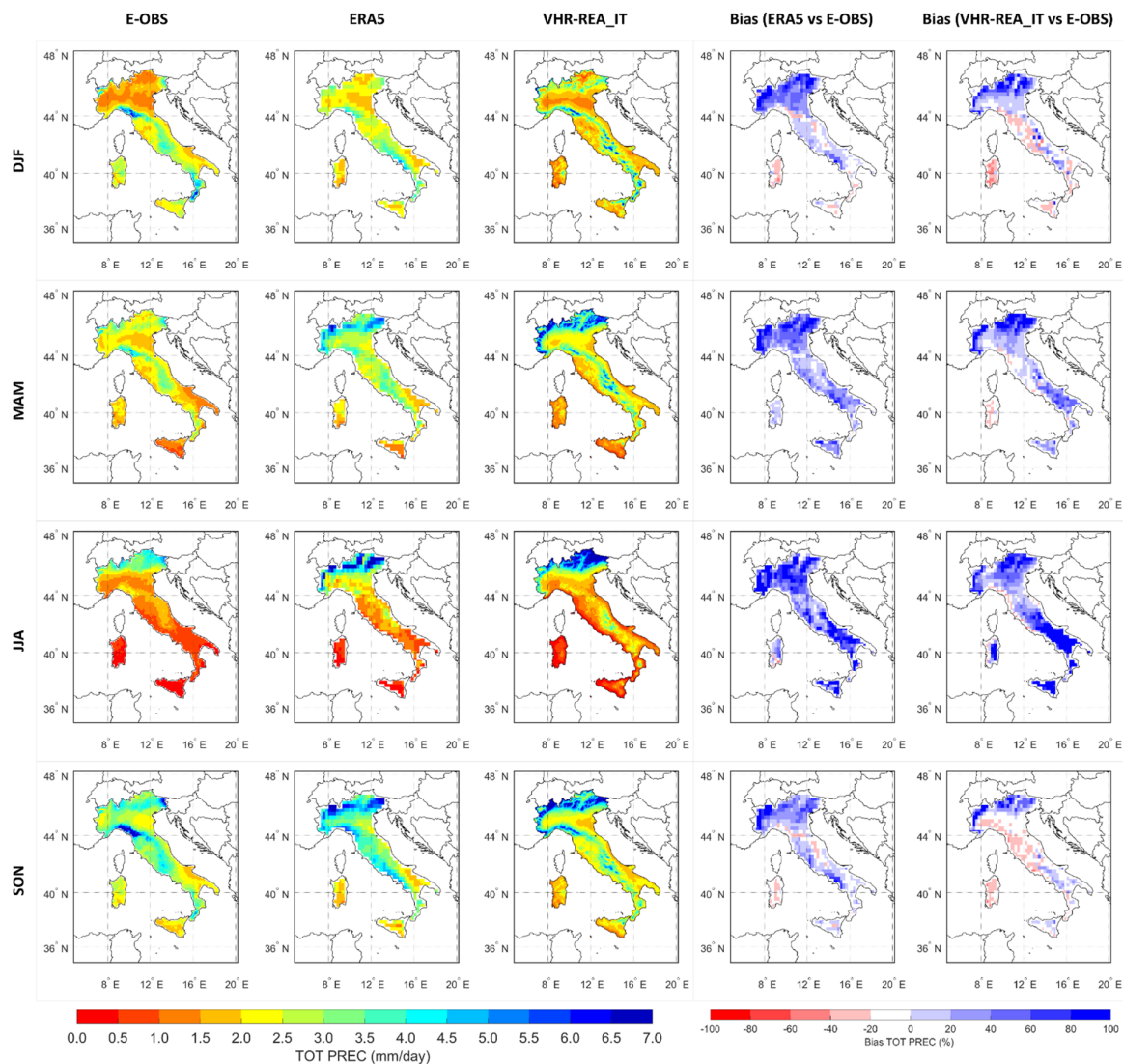


**Figure 3.** The first three columns: Seasonal (in row) spatial distribution of daily precipitation for the period 1989–2020 provided by E-OBS, ERA5, and VHR-REA\_IT (in column); the last two columns: Seasonal (in row) spatial distribution of daily precipitation bias for the period 1989–2020 provided by ERA5 and VHR-REA\_IT (in column), assuming E-OBS as a reference.

Additionally, in this case, to support the validation activity and provide a more comprehensive overview, a summary of results for different areas is reported in Table 7.

**Table 7.** Seasonal mean precipitation analysis for the period 1989–2020 provided by E-OBS, ERA5, and VHR-REA\_IT. Data are aggregated over Italy and consider the five subareas identified in Figure 1b. For E-OBS, reference values are reported in italic and bold (units = mm/day); for ERA5 and VHR-REA\_IT, percent bias ( $100 * (\text{mod} - \text{obs}) / \text{obs}$ ) and ratio between the standard deviation ( $\sigma_{\text{mod}} / \sigma_{\text{obs}}$ ) are reported. The colors are used to classify differences.

|                 |            | Bias (%)    |             |             |             | $\sigma_{\text{mod}} / \sigma_{\text{obs}}$ |             |             |             |
|-----------------|------------|-------------|-------------|-------------|-------------|---|-------------|-------------|-------------|
|                 |            | DJF         | MAM         | JJA         | SON         | DJF   | MAM         | JJA         | SON         |
| Italy           | E-OBS      | <b>2.27</b> | <b>2.15</b> | <b>1.44</b> | <b>3.02</b> | <b>0.88</b>                                 | <b>0.70</b> | <b>1.09</b> | <b>0.97</b> |
|                 | ERA5       | 12%         | 33%         | 50%         | 17%         | 0.7   | 1.5         | 1.7         | 1.3         |
|                 | VHR-REA_IT | 0%          | 24%         | 42%         | −2%         | 1.1   | 1.9         | 1.6         | 1.4         |
| Northwest Italy | E-OBS      | <b>1.91</b> | <b>2.42</b> | <b>2.15</b> | <b>3.40</b> | <b>0.39</b>                                 | <b>0.22</b> | <b>0.18</b> | <b>0.37</b> |
|                 | ERA5       | 30%         | 51%         | 70%         | 31%         | 0.5   | 1.4         | 2.9         | 1.2         |
|                 | VHR-REA_IT | 29%         | 51%         | 42%         | 22%         | 0.7   | 1.6         | 1.5         | 0.9         |
| Northeast Italy | E-OBS      | <b>1.78</b> | <b>2.37</b> | <b>2.52</b> | <b>3.27</b> | <b>0.38</b>                                 | <b>0.26</b> | <b>0.21</b> | <b>0.50</b> |
|                 | ERA5       | 30%         | 39%         | 42%         | 20%         | 0.6   | 1.2         | 3.1         | 0.9         |
|                 | VHR-REA_IT | 27%         | 44%         | 43%         | 9%          | 1.1   | 1.5         | 2.0         | 0.9         |
| Central Italy   | E-OBS      | <b>2.97</b> | <b>2.56</b> | <b>1.24</b> | <b>3.86</b> | <b>0.24</b>                                 | <b>0.16</b> | <b>0.08</b> | <b>0.27</b> |
|                 | ERA5       | 1%          | 11%         | 16%         | 3%          | 0.8   | 1.2         | 1.8         | 1.0         |
|                 | VHR-REA_IT | −15%        | −4%         | 11%         | −24%        | 1.1   | 1.6         | 2.7         | 0.7         |
| South Italy     | E-OBS      | <b>3.01</b> | <b>2.06</b> | <b>0.77</b> | <b>2.83</b> | <b>0.30</b>                                 | <b>0.17</b> | <b>0.09</b> | <b>0.19</b> |
|                 | ERA5       | −1%         | 23%         | 61%         | 6%          | 0.9   | 1.2         | 1.9         | 2.0         |
|                 | VHR-REA_IT | −9%         | 17%         | 86%         | −9%         | 1.3   | 2.0         | 3.0         | 1.5         |
| Insular Italy   | E-OBS      | <b>2.39</b> | <b>1.47</b> | <b>0.33</b> | <b>2.21</b> | <b>0.12</b>                                 | <b>0.09</b> | <b>0.02</b> | <b>0.08</b> |
|                 | ERA5       | −10%        | 15%         | 29%         | −5%         | 1.0   | 1.2         | 3.7         | 1.8         |
|                 | VHR-REA_IT | −28%        | −12%        | 42%         | −22%        | 2.5   | 1.7         | 6.2         | 2.2         |

Bias (%)

$\sigma_{\text{mod}} / \sigma_{\text{obs}}$

Mean precipitation observations are in general reduced during summer (1.44 mm/day) and relevant during autumn (3.02 mm/day). By looking at Table 7, these values are different in the various areas; specifically, the northern part also exhibits high precipitation during summer while the southern part, as well as the insular area, are rather dry. In comparison with observations, ERA5 tends to increase precipitation across Italy, especially during spring and summer; conversely, the spatial refinement of ERA5 at 2.2 km reduces this wet bias providing values in line with observations, with some exceptions in central, southern, and insular Italy. It is of interest to show how VHR-REA\_IT increases summer precipitation against ERA as expected for CP models excepting for Northwest Italy and Central Italy. This is evident, especially in Southern Italy (bias = +86%). Moreover, in terms of spatial variability, the ratio between the standard deviation of RCM data and observations increases, moving from ERA5 to VHR-REA\_IT as the refinement of spatial resolution reduces the smoothing of precipitation.

### 3.1.3. Climate Indicators Evaluation

This section provides an overview about extremes considering climate indicators listed in Tables 4 and 5. Specifically, these indicators are computed with E-OBS, ERA5, and VHR-REA\_IT for each grid cell considering datasets in their native resolution and then aggregated at different spatial units (i.e., over Italy and for the five subareas reported in

Figure 1b). The results are reported in Table 8 for indicators derived from temperature and Table 9 for indicators derived from precipitation.

**Table 8.** List of considered indicators related to temperature.

|                    |            | ID<br>(Days/Year) | SU<br>(Days/Year) | FD<br>(Days/Year) | TR<br>(Days/Year) | TXx (°C) | 90p tmax<br>(°C) | 10p tmin<br>(°C) | TNn<br>(°C) |
|--------------------|------------|-------------------|-------------------|-------------------|-------------------|----------|------------------|------------------|-------------|
| Italy              | E-OBS      | 8                 | 89                | 41                | 25                | 33.6     | 28.2             | 1.1              | −4.9        |
|                    | ERA5       | 10                | 75                | 42                | 32                | 32.4     | 27.3             | 1.0              | −5.5        |
|                    | VHR-REA_IT | 12                | 106               | 34                | 54                | 36.6     | 30.5             | 1.7              | −4.9        |
| Northwest<br>Italy | E-OBS      | 21                | 59                | 90                | 7                 | 30.1     | 25.3             | −3.3             | −9.6        |
|                    | ERA5       | 33                | 39                | 99                | 11                | 28.6     | 23.8             | −4.8             | −12.5       |
|                    | VHR-REA_IT | 35                | 71                | 79                | 35                | 32.4     | 27.1             | −2.6             | −9.3        |
| Northeast<br>Italy | E-OBS      | 20                | 72                | 91                | 11                | 31.7     | 26.5             | −3.5             | −10.3       |
|                    | ERA5       | 24                | 57                | 86                | 20                | 30.9     | 25.7             | −3.8             | −11.4       |
|                    | VHR-REA_IT | 27                | 84                | 69                | 43                | 34.3     | 28.7             | −2.2             | −9.1        |
| Central<br>Italy   | E-OBS      | 2                 | 94                | 31                | 13                | 34.4     | 29.4             | 0.9              | −5.2        |
|                    | ERA5       | 1                 | 75                | 29                | 22                | 32.4     | 27.9             | 1.5              | −5.1        |
|                    | VHR-REA_IT | 4                 | 110               | 23                | 49                | 37.0     | 31.5             | 1.8              | −5.3        |
| South<br>Italy     | E-OBS      | 1                 | 96                | 20                | 29                | 34.9     | 29.3             | 2.5              | −3.3        |
|                    | ERA5       | 1                 | 79                | 21                | 36                | 33.0     | 27.9             | 2.9              | −3.5        |
|                    | VHR-REA_IT | 4                 | 110               | 18                | 60                | 37.5     | 31.2             | 3.0              | −3.8        |
| Insular<br>Italy   | E-OBS      | 0                 | 108               | 1                 | 45                | 34.9     | 29.6             | 5.7              | 0.8         |
|                    | ERA5       | 0                 | 102               | 5                 | 52                | 34.5     | 29.3             | 5.7              | 0.8         |
|                    | VHR-REA_IT | 0                 | 126               | 4                 | 73                | 38.6     | 31.9             | 6.0              | 0.1         |

**Table 9.** List of considered indicators related to precipitation.

|                    |            | CDD<br>(Days/Year) | CWD<br>(Days/Year) | Rx1day<br>(mm/Day) | Rx5day<br>(mm/5<br>Days) | 90p<br>(mm/Day) | 99p<br>(mm/Day) | R10<br>(Days/Year) | R20<br>(Days/Year) |
|--------------------|------------|--------------------|--------------------|--------------------|--------------------------|-----------------|-----------------|--------------------|--------------------|
| Italy              | E-OBS      | 47                 | 8                  | 47.3               | 93.5                     | 19.4            | 44.0            | 26                 | 8                  |
|                    | ERA5       | 32                 | 10                 | 48.7               | 94.6                     | 16.9            | 40.5            | 28                 | 9                  |
|                    | VHR-REA_IT | 42                 | 7                  | 64.0               | 106.4                    | 22.7            | 56.9            | 27                 | 11                 |
| Northwest<br>Italy | E-OBS      | 34                 | 8                  | 53.5               | 109.8                    | 21.2            | 48.8            | 30                 | 10                 |
|                    | ERA5       | 21                 | 12                 | 64.8               | 132.1                    | 20.5            | 51.2            | 38                 | 15                 |
|                    | VHR-REA_IT | 30                 | 8                  | 77.1               | 144.7                    | 27.0            | 65.5            | 37                 | 17                 |
| Northeast<br>Italy | E-OBS      | 32                 | 8                  | 48.3               | 98.1                     | 20.2            | 43.3            | 30                 | 10                 |
|                    | ERA5       | 22                 | 11                 | 53.7               | 106.0                    | 19.0            | 43.2            | 37                 | 13                 |
|                    | VHR-REA_IT | 28                 | 8                  | 64.3               | 115.2                    | 24.0            | 54.7            | 38                 | 16                 |
| Central<br>Italy   | E-OBS      | 36                 | 8                  | 56.7               | 110.9                    | 22.7            | 50.7            | 33                 | 12                 |
|                    | ERA5       | 25                 | 10                 | 50.8               | 99.4                     | 18.8            | 42.4            | 33                 | 11                 |
|                    | VHR-REA_IT | 37                 | 6                  | 60.1               | 98.7                     | 22.5            | 52.9            | 27                 | 11                 |
| South<br>Italy     | E-OBS      | 45                 | 8                  | 46.3               | 92.8                     | 18.9            | 43.3            | 26                 | 8                  |
|                    | ERA5       | 29                 | 9                  | 48.3               | 93.7                     | 16.1            | 39.6            | 26                 | 8                  |
|                    | VHR-REA_IT | 38                 | 6                  | 68.9               | 110.4                    | 22.8            | 60.0            | 25                 | 10                 |
| Insular<br>Italy   | E-OBS      | 71                 | 7                  | 42.9               | 79.3                     | 17.7            | 41.5            | 19                 | 5                  |
|                    | ERA5       | 52                 | 7                  | 37.8               | 68.9                     | 13.9            | 33.9            | 16                 | 4                  |
|                    | VHR-REA_IT | 67                 | 5                  | 53.0               | 79.5                     | 19.4            | 52.3            | 14                 | 5                  |

In general, the analysis of extreme climate indicators reflects the tendency of VHR-REA\_IT to amplify climate dynamics due to the spatial resolution refinement.

#### 4. User Notes

The dataset VHR-REA\_IT aims to provide a set of unprecedented high-quality and very high-resolution historical climate data. It allows users to assess recent trends in average and extreme climatic conditions that led to numerous cascading hazards over the land surface and connected sectors. Typical use of this dataset is research and downstream services, e.g., for decision support systems in different sectors highly affected by changes in climate trends, variability, and extreme events, as in the case of Italy. For example, starting from the time series of climate data, process-based hydrological modelling can be applied to

simulate water cycle components, like evapotranspiration, soil moisture, and runoff up to discharge, and to produce indicators of meteorological–hydrological–agricultural drought attributes, i.e., frequency, magnitude, duration, and timing. The same time series can drive crop or forest growth models assessing vegetation productivity through reproduction of carbon, water, and energy exchanges, as well as feed fire hazard indicators and fire behavior simulations. Last but not least, diurnal, seasonal to interannual variability of extreme conditions can help in assessing changes to dangerous conditions for people and animals, allowing us to discriminate between rural and urban environments thanks to the high spatial resolution implemented.

The VHR-REA\_IT dataset features some limitations that must be properly considered for correct use. Although it is obtained by dynamically downscaling a reanalysis (i.e., ERA5), some biases may be noticed due to the absence of a data assimilation procedure, which, considering the resolution of this new dataset, is hard to include over all domains with the same characteristic.

In this sense, it is also important to stress how the use of an urban parameterization such as TERRA-URB correctly leads to an increasing of temperature over urban centers. Such an increase is hard to detect by ERA5 reanalysis or E-OBS observations due to their resolution (at least five times lower for E-OBS and 15 times lower for ERA5). It could be evaluated against observations provided by urban meteorological stations. However, these measurements are hard to retrieve as synoptic stations are often used.

To sum up, some biases may be encountered; they should be evaluated with punctual observations and appropriately removed through bias correction procedures to correctly feed impact models.

**Author Contributions:** Conceptualization, P.M.; methodology, M.R. and P.M.; software, M.R. and M.M.; validation, M.R., and A.R.; formal analysis, M.R.; investigation, P.M. and A.R.; resources, G.F.M.; data curation, M.R. and M.M.; writing—original draft preparation, A.R. and M.R.; writing—review and editing, P.M., M.S., M.M., G.F.M. and G.S.; visualization, M.R.; supervision, P.M. and M.S.; project administration, G.S.; funding acquisition, G.S. and M.S. All authors have read and agreed to the published version of the manuscript.

**Funding:** This research was funded by the HIGHLANDER (HIGH performance computing to support smart LAND sERVICES) project, which is funded by the Connecting European Facility (CEF) Telecommunications sector under agreement number INEA/CEF/ICT/A2018/1815462.

**Data Availability Statement:** The study produced an extensive dataset that can be accessed at [https://doi.org/10.25424/cmcc/era5-2km\\_italy](https://doi.org/10.25424/cmcc/era5-2km_italy).

**Acknowledgments:** The experiments were performed using the COSMO model in CLimate Mode (COSMO-CLM). COSMO-CLM is the community model of the German regional climate research team, jointly further developed by the CLM-Community. We acknowledge the members of the community for their common efforts to develop the model and to find the right setups. Finally, we acknowledge the E-OBS dataset from the EU-FP6 project UERRA (<http://www.uerra.eu>), the Copernicus Climate Change Service, and the data providers in the ECA&D project (<https://www.ecad.eu>).

**Conflicts of Interest:** The authors declare no conflict of interest.

## References

1. Kendon, E.J.; Prein, A.F.; Senior, C.A.; Stirling, A. Challenges and outlook for convection-permitting climate modelling. *Philos. Trans. R. Soc.* **2021**, *379*, 20190547. [[CrossRef](#)] [[PubMed](#)]
2. Ban, N.; Schmidli, J.; Schär, C. Evaluation of the new convective-resolving regional climate modelling approach in decade-long simulations. *J. Geophys. Res. Atmos.* **2014**, *119*, 7889–7907. [[CrossRef](#)]
3. Berthou, S.; Kendon, E.J.; Chan, S.C.; Ban, N.; Leutwyler, D.; Schär, C.; Fosser, G. Pan-European climate at convection-permitting scale: A model intercomparison study. *Clim. Dyn.* **2018**, *5*, 1–25. [[CrossRef](#)]
4. Coppola, E.; Sobolowski, S.; Pichelli, E.; Raffaele, F.; Ahrens, B.; Anders, I.; Ban, N.; Bastin, S.; Belda, M.; Belušić, D.; et al. A first-of-its-kind multi-model convection permitting ensemble for investigating convective phenomena over Europe and the Mediterranean. *Clim. Dyn.* **2020**, *55*, 3–34. [[CrossRef](#)]

5. Fumière, Q.; Déqué, M.; Nuissier, O.; Somot, S.; Alias, A.; Caillaud, C.; Laurantin, O.; Seity, Y. Extreme rainfall in Mediterranean France during the fall: Added-value of the CNRM-AROME convection permitting regional climate model. *Clim. Dyn.* **2020**, *55*, 77–91. [[CrossRef](#)]
6. Fossier, G.; Khodayar, S.; Berg, P. Benefit of convection permitting climate model simulations in the representation of convective precipitation. *Clim. Dyn.* **2015**, *44*, 45–60. [[CrossRef](#)]
7. Prein, A.F.; Langhans, W.; Fossier, G.; Ferrone, A.; Ban, N.; Goergen, K.; Keller, M.; Toelle, M.; Gutjahr, O.; Feser, F.; et al. A review on regional convection-permitting climate modeling: Demonstrations, prospects, and challenges. *Rev. Geophys.* **2015**, *53*, 323–361. [[CrossRef](#)]
8. Piazza, M.; Prein, A.F.; Truhetz, H.; Csaki, A. On the sensitivity of precipitation in convection-permitting climate simulations in the Eastern Alpine region. *Meteorol. Z.* **2019**, *28*, 323–346. [[CrossRef](#)]
9. Adinolfi, M.; Raffa, M.; Reder, A.; Mercogliano, P. Evaluation and Expected Changes of Summer Precipitation at Convection Permitting Scale with COSMO-CLM over Alpine Space. *Atmosphere* **2020**, *12*, 54. [[CrossRef](#)]
10. Raffa, M.; Reder, A.; Adinolfi, M.; Mercogliano, P. A Comparison between One-Step and Two-Step Nesting Strategy in the Dynamical Downscaling of Regional Climate Model COSMO-CLM at 2.2 km Driven by ERA5 Reanalysis. *Atmosphere* **2021**, *12*, 260. [[CrossRef](#)]
11. Ban, N.; Caillaud, C.; Coppola, E.; Pichelli, E.; Sobolowski, S.; Adinolfi, M.; Ahrens, B.; Alias, A.; Anders, I.; Bastin, S.; et al. The first multi-model ensemble of regional climate simulations at kilometer-scale resolution, part I: Evaluation of precipitation. *Clim. Dyn.* **2021**, *57*, 275–302. [[CrossRef](#)]
12. Fowler, H.J.; Wasko, C.; Prein, A.F. Intensification of short-duration rainfall extremes and implications for flood risk: Current state of the art and future directions. *Philos. Trans. R. Soc. A: Math. Phys. Eng. Sci.* **2021**, *379*, 20190541. [[CrossRef](#)]
13. Reder, A.; Raffa, M.; Montesarchio, M.; Mercogliano, P. Performance evaluation of regional climate model simulations at different spatial and temporal scales over the complex orography area of the Alpine region. *Nat. Hazards* **2020**, *102*, 151–177. [[CrossRef](#)]
14. Taylor, C.; Birch, C.E.; Parker, D.; Dixon, N.; Guichard, F.; Nikulin, G.; Lister, G.M.S. Modeling soil moisture-precipitation feedback in the Sahel: Importance of spatial scale versus convective parameterization. *Geophys. Res. Lett.* **2013**, *40*, 6213–6218. [[CrossRef](#)]
15. Trusilova, K.; Früh, B.; Brienen, S.; Walter, A.; Masson, V.; Pigeon, G.; Becker, P. Implementation of an Urban Parameterization Scheme into the Regional Climate Model COSMO-CLM. *J. Appl. Meteorol. Climatol.* **2013**, *52*, 2296–2311. [[CrossRef](#)]
16. Hersbach, H.; Bell, B.; Berrisford, P.; Hirahara, S.; Horanyi, A.; Muñoz-Sabater, J.; Nicolas, J.; Peubey, C.; Radu, R.; Schepers, D.; et al. The ERA5 global reanalysis. *Q. J. R. Meteorol. Soc.* **2020**, *146*, 1999–2049. [[CrossRef](#)]
17. Buontempo, C.; Hutjes, R.; Beavis, P.; Berckmans, J.; Cagnazzo, C.; Vamborg, F.; Thépaut, J.-N.; Bergeron, C.; Almond, S.; Amici, A.; et al. Fostering the development of climate services through Copernicus Climate Change Service (C3S) for agriculture applications. *Weather. Clim. Extremes* **2020**, *27*, 100226. [[CrossRef](#)]
18. UCAR/Unidata Program Center. *Unidata, Network Common Data Form (NetCDF), V4.8.0*; UCAR/Unidata Program Center: Boulder, CO, USA, 2019.
19. Cornes, R.C.; Van Der Schrier, G.; Besselaar, E.V.D.; Jones, P.D. An Ensemble Version of the E-OBS Temperature and Precipitation Data Sets. *J. Geophys. Res. Atmos.* **2018**, *123*, 9391–9409. [[CrossRef](#)]
20. Rockel, B.; Will, A.; Hense, A. The Regional Climate Model COSMO-CLM (CCLM). *Meteorol. Z.* **2008**, *17*, 347–348. [[CrossRef](#)]
21. Wouters, H.; Demuzere, M.; Blahak, U.; Fortuniak, K.; Maiheu, B.; Camps, J.; Tielemans, D.; van Lipzig, N.P.M. The efficient urban canopy dependency parametrization (SURY) v1.0 for atmospheric modelling: Description and application with the COSMO-CLM model for a Belgian summer. *Geosci. Model. Dev.* **2016**, *9*, 3027–3054. [[CrossRef](#)]
22. Ritter, B.; Geleyn, J.F. A comprehensive radiation scheme for numerical weather prediction models with potential applications in climate simulations. *Mon. Weather Rev.* **1992**, *120*, 303–325. [[CrossRef](#)]
23. Tiedtke, M. A comprehensive mass flux scheme for cumulus parameterization in large-scale models. *Mon. Weather Rev.* **1989**, *117*, 1779–1800. [[CrossRef](#)]
24. Doms, G.; Forstner, J.; Heise, E.; Herzog, H.J.; Mironov, D.; Raschendorfer, T.; Reinhardt, T.; Ritter, B.; Schrodin, R.; Schulz, J.P.; et al. A Description of the Non-Hydrostatic Regional COSMO Model. Part-II: Physical Parameterization. 2011. Available online: <https://klimanavigator.eu/imperia/md/content/csc/klimanavigator/cosmophysparamtr.pdf> (accessed on 23 December 2020).
25. Baldauf, M.; Schulz, J.P. *Prognostic precipitation in the lokal modell (LM) of DWD*. COSMO Newsletter No. 4.; Deutscher Wetterdienst: Offenbach am Main, Germany, 2004; pp. 177–180.
26. Bartholomé, E.; Belward, A.S. GLC2000: A new approach to global land cover mapping from Earth observation data. *Int. J. Remote. Sens.* **2005**, *26*, 1959–1977. [[CrossRef](#)]
27. Mellor, G.L.; Yamada, T. A hierarchy of turbulence closure models for planetary boundary layers. *J. Atmos. Sci.* **1974**, *31*, 1791–1806. [[CrossRef](#)]
28. Giorgi, F.; Gutowski, W.J. Regional Dynamical Downscaling and the CORDEX Initiative. *Annu. Rev. Environ. Resour.* **2015**, *40*, 467–490. [[CrossRef](#)]
29. Jacob, D.; Petersen, J.; Eggert, B.; Alias, A.; Christensen, O.B.; Bouwer, L.M.; Braun, A.; Colette, A.; Déqué, M.; Georgievski, G.; et al. EURO-CORDEX: New high-resolution climate change projections for European impact research. *Reg. Environ. Chang.* **2014**, *14*, 563–578. [[CrossRef](#)]
30. Padulano, R.; Rianna, G.; Santini, M. Datasets and approaches for the estimation of rainfall erosivity over Italy: A comprehensive comparison study and a new method. *J. Hydrol. Reg. Stud.* **2021**, *34*, 100788. [[CrossRef](#)]

- 
31. Haylock, M.R.; Hofstra, N.; Tank, A.K.; Klok, E.J.; Jones, P.; New, M. A European daily high-resolution gridded data set of surface temperature and precipitation for 1950–2006. *J. Geophys. Res. Space Phys.* **2008**, *113*. [[CrossRef](#)]
  32. Prein, A.F.; Gobiet, A. Impacts of uncertainties in European gridded precipitation observations on regional climate analysis. *Int. J. Clim.* **2017**, *37*, 305–327. [[CrossRef](#)]
  33. Isotta, F.A.; Frei, C.; Weilguni, V.; Tadić, M.P.; Lassègues, P.; Rudolf, B.; Pavan, V.; Cacciamani, C.; Antolini, G.; Ratto, S.M.; et al. The climate of daily precipitation in the Alps: Development and analysis of a high-resolution grid dataset from pan-Alpine rain-gauge data. *Int. J. Clim.* **2013**, *34*, 1657–1675. [[CrossRef](#)]